Asymptotic fields for a Hamiltonian treatment of nonlinear electromagnetic phenomena

M. Liscidini
Dipartimento di Fisica "Alessandro Volta," Università degli Studi di Pavia, via Bassi 6, I-27100 Pavia, Italy

L. G. Helt and J. E. Sipe
Department of Physics and Institute for Optical Sciences, University of Toronto, 60 St. George Street, Ontario, Canada M5S 1A7
(Received 20 October 2011; published 23 January 2012)

We discuss the use of asymptotic-in and -out fields in a Hamiltonian treatment of nonlinear electromagnetic problems. Our approach allows a description of nonlinear phenomena in a number of geometries and is suitable to treat integrated photonic structures, particularly cavities. We present examples in which the nonlinear phenomena are weak enough for pump depletion to be neglected, and we report some results related to the description of second-order nonlinear processes in ring resonators and layered structures.

DOI: 10.1103/PhysRevA.85.013833 PACS number(s): 42.65.Lm, 42.65.Wi

I. INTRODUCTION

Optical cavities and their properties play a central role in photonics. In classical linear optics, they arise in the development of slow-light structures [1], where it has recently been suggested that novel designs can lead to robust delay lines that are topologically protected [2]. In quantum optics, the Purcell effect [3] has enabled a host of exciting developments in the control of spontaneous emission and has served as the paradigmatic example of the effect of the environment on the optical properties of material systems. In nonlinear optics, the role of cavities in confining light and enhancing electromagnetic fields has inspired developments in fields ranging from optical bistability [4,5], to all-optical switching [6–8], to harmonic generation [9–12], to the use of light both to drive mechanical resonances and to cool them to their quantum limit [13]. Similarly, photonic crystal waveguides, which can be viewed as open cavities, are promising platforms for the enhancement of nonlinear optics phenomena using slow light [14]. With this wide-ranging interest in optical cavities, it is perhaps not surprising that they are being investigated for use in the enhancement of processes in nonlinear quantum optics [15–19], such as the generation of quantum correlated pairs of photons by either spontaneous parametric down-conversion (SPDC) or spontaneous four-wave mixing.

In such applications, where a fully quantum treatment of the electromagnetic field is desired, the natural starting point would be a linear Hamiltonian that involves cavity modes, modes of the electromagnetic field that can carry energy to and away from the cavity, and a coupling Hamiltonian between them. Such a Hamiltonian is often referred to as a *Gardiner-Collett Hamiltonian* [20], and was used by those authors in their treatment of damped quantum systems [21]. In some structures this approach can be easily implemented. For example, in the coupling of a waveguide channel to a ring resonator the coupling is often idealized as occurring at a single point [see Fig. 1(a)] [22]. Within this approximation, it is straightforward to build an effective Hamiltonian of the Gardiner-Collet type that models the optics of the resonator and channel [15,17]. However, the problem is nontrivial for other cavity structures, such as even a simple one-dimensional (1D) Fabry-Pérot cavity. There is a large literature about how quasimodes can be introduced for a Fabry-Pérot cavity and their coupling with the outside world described [23]; a review of the history of the subject, and a very careful approach to the problem, has been presented by Dutra [20]. A careful analysis of more complicated structures even in one dimension, such as the photonic crystal cavity shown in Fig. 1(b), would certainly be more difficult. In more complex structures such as that indicated schematically in Fig. 2 the problem would be even worse.

A different strategy harks back to the elementary theory of scattering in quantum mechanics. There one can introduce *asymptotic-in* and *asymptotic-out*states, as was done in the classic paper of Breit and Bethe [24]. These are full solutions of the (linear) Schrödinger equation, including the scattering potential, and exist everywhere in space. But they are built so that a natural superposition of them corresponds to an incident wave packet at $t = -\infty$ (asymptotic-in), or an exiting wave packet at $t = \infty$ (asymptotic-out) [25]. In elementary quantum mechanics the construction of these states constitutes a solution of the scattering problem itself. In photonics the construction of the corresponding solutions of the linear Maxwell equations for a structure such as that in Fig. 2, which can often be found numerically even if not analytically, constitutes a solution of only the *linear* scattering problem. Indeed, as we show in detail below, that linear scattering problem can be encapsulated in a transformation from the asymptotic-in to the asymptotic-out fields. However, those fields also form the natural basis for the treatment of a nonlinear optics problem, especially if the nonlinearity can be idealized as restricted to an "interaction" region as indicated schematically in Fig. 2; in the particular examples of Figs. 1(a) and 1(b) this would correspond to the ring or the photonic crystal structure.

In this strategy there is no introduction of artificial "cavity modes," which of course do not really exist in structures such as those shown in Figs. 1(a) and 1(b). The enhancement of nonlinear optical effects due to the time light spends in a cavitylike structure (such as the ring or photonic crystal structure in our two examples) is completely captured by the distribution of the asymptotic-in and asymptotic-out fields. Hence the problem of trying to correctly identify approximate quasimodes and their effective coupling to input and output channels is completely bypassed. We will see that the

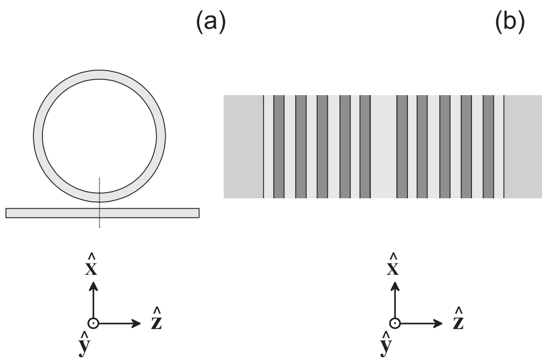

FIG. 1. A sketch of (a) a ring resonator and (b) a one-dimensional planar microcavity.

strategy we develop here simplifies not only quantum optics calculations but even more traditional calculations in classical nonlinear optics.

While earlier work has anticipated some aspects of what we present here in optics [26,27], and analogous approaches have arisen in the treatment of electron transport in channels and cavitylike structures [28], here we develop a general framework for problems in nonlinear quantum optics. The formalism can consider single-particle states, as in elementary quantum scattering theory, as well as more complicated states including coherent states, squeezed vacua, and Fock states. Additionally, both the material and modal dispersion of the input and output channels, such as those sketched in Fig. 2, can be important in the analysis of real artificially structured materials; our approach can include them very naturally. Scattering of light out of the structure and absorption losses are sometimes also important, but we defer their inclusion to later presentations.

In Sec. II we introduce some terminology for the generic structure sketched in Fig. 2. The linear optics of such a structure is considered in Sec. III, where we introduce the asymptotic-in and -out fields at the classical level and then turn to the quantization of these fields. Conditions on the transmission coefficients are derived, and the natural treatment of linear scattering in terms of these fields is presented in the simple case of coherent states incident on the interaction region. In Sec. IV we formulate the general scattering problem in the presence of nonlinearities in terms of the asymptotic-in and -out fields and give two examples in the following two sections. In Sec. V we consider the ring resonator of Fig. 1(a), where we show that this strategy easily reproduces the usual results obtained with a Gardiner-Collett Hamiltonian for SPDC. In Sec. VI we consider a photonic crystal structure and show that our theory reproduces the results for classical second harmonic generation (SHG) with more ease than the traditional calculation. We demonstrate that the same formalism can also be employed to predict both the SPDC efficiency and the biphoton wave function characterizing the entangled photons generated. Our conclusions are presented in Sec. VII.

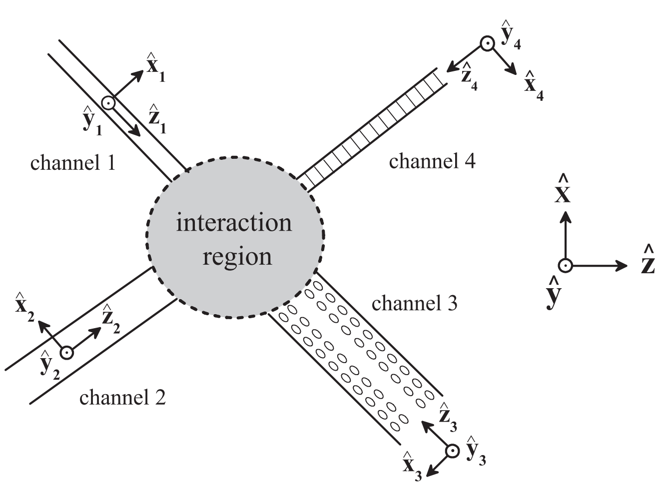

FIG. 2. A sketch of the kind of structure of interest. The origin of the laboratory frame is at the center of the interaction region, which is where the local z coordinates of the channels take the value 0.

II. STRUCTURES OF INTEREST

We consider structures of the form indicated schematically in Fig. 2, where there are a number of channels connected by an interaction region. The channels could all be of the same type, or of different types, as indicated in the figure. They can also be understood more generally than the ridge and photonic waveguides that are sketched, as we will see later. However, it will be useful to adopt the language appropriate for the kinds of channels sketched in Fig. 2 to fix the notation. The only really important assumption is that these channels identify all the ways that energy can move toward or away from the interaction region, i.e., all pathways of any significance are taken into account; we plan to generalize this to include absorption and scattering losses in a later presentation. We leave the details of the interaction region, indicated only in "cartoon fashion" by the central circular region, unspecified for the moment. When we include nonlinear effects we will assume they arise only in the interaction region.

Associated with each channel we indicate a local coordinate system, with unit vectors $\hat{\mathbf{x}}_n$, $\hat{\mathbf{y}}_n$, and $\hat{\mathbf{z}}_n$, where n identifies the channel. The orientation of these vectors is restricted only in that each of the $\hat{\mathbf{z}}_n$ points *toward* the interaction region, and the values $z_n = 0$ occur at a point that would lie near the center of the interaction region. We denote the coordinates of a position vector in one of these local frames by $\mathbf{r}_n = (x_n, y_n, z_n)$, reserving $\mathbf{r} = (x, y, z)$ to denote the coordinates in a laboratory frame, placing $\mathbf{r} = \mathbf{0}$ at the center of the interaction region.

It is clear from Fig. 2 that we assume each channel must "end" at a certain point, either at the boundary of the interaction region or somewhere within it. So below when we indicate functions of $\mathbf{r}_n$, $f(\mathbf{r}_n)$, what we mean are such functions truncated at the ending point of the indicated channel. That is, we take $f(\mathbf{r}_n)$ to really mean

$$f(\mathbf{r}_n) \rightarrow f(\mathbf{r}_n)\theta(D_n - z_n), \tag{1}$$

where θ is the usual step function, $\theta(z) = 0$ when $z < 0$ and $\theta(z) = 1$ when $z > 0$, and D_n is a (negative) number (recalling the definition of $z_n = 0$) that indicates the end of the channel. Functions of $\mathbf{r}$, on the other hand, are taken to be defined everywhere in space.

We also consider individual channels that carry on infinitely in the local propagation direction, but are of the same type

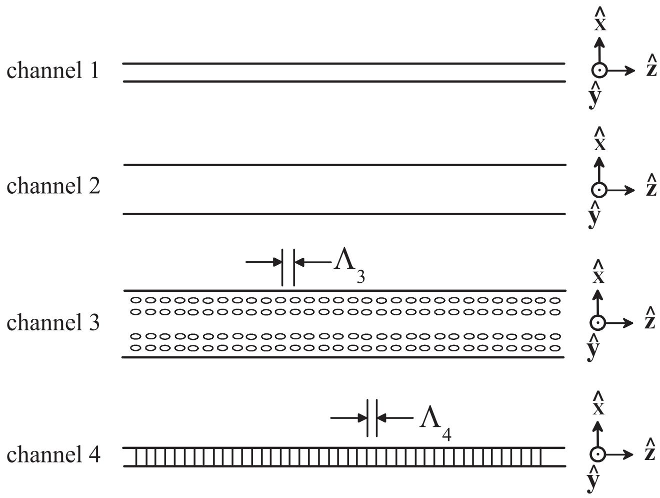

FIG. 3. The channels are assumed infinite in length and separated far enough from each other that they can be considered isolated.

as the channels appearing in our actual structure. These are shown schematically in Fig. 3, and are to be imagined far enough apart so they can be considered as isolated systems. When considering these isolated channels we simply use $\hat{\mathbf{x}}$, $\hat{\mathbf{y}}$, and $\hat{\mathbf{z}}$ to indicate the unit vectors, with $\hat{\mathbf{z}}$ pointing along the propagation direction.

Returning to Fig. 2, we see that as $|\mathbf{r}|$ increases the distance between the channels also increases. In writing general functions of $\mathbf{r}$, $F(\mathbf{r})$, we use $F(\mathbf{r}) \sim \cdots$ to indicate that $|\mathbf{r}|$ is large enough so that the channels can be taken to be isolated, with $\cdots$ then a good approximation of $F(\mathbf{r})$.

III. LINEAR OPTICS OF THE STRUCTURES

We begin by neglecting the presence of any nonlinearity, and formulate both classical and quantum descriptions of the linear optical properties of our structures.

A. Asymptotic-in and -out fields

A starting point for our calculations will be the classical optics of the isolated channels sketched in Fig. 3. Since the displacement field $\mathbf{D}(\mathbf{r},t)$ and the magnetic field $\mathbf{B}(\mathbf{r},t)$ are divergenceless, it is useful to consider them as our fundamental fields. We imagine that the modes of a particular channel n are found and will be labeled by a discrete index I and a continuous index k, with frequency $\omega_{nIk} > 0$; we denote the displacement and magnetic *mode fields* as $\mathbf{D}_{nIk}(\mathbf{r})$ and $\mathbf{B}_{nIk}(\mathbf{r})$ respectively, so that the electromagnetic field in a set of isolated channels as shown in Fig. 2 can be written as

$$\mathbf{D}(\mathbf{r},t) = \sum_{n,I\epsilon\sigma_n} \int_{-\infty}^{\infty} dk\, \gamma_{nIk} e^{-i\omega_{nIk}t}\mathbf{D}_{nIk}(\mathbf{r}) + \text{c.c.},$$
$$\mathbf{B}(\mathbf{r},t) = \sum_{n,I\epsilon\sigma_n} \int_{-\infty}^{\infty} dk\, \gamma_{nIk} e^{-i\omega_{nIk}t}\mathbf{B}_{nIk}(\mathbf{r}) + \text{c.c.}, \tag{2}$$

with complex mode amplitudes γ_{nIk}; we use σ_n to specify the set of modes allowed in channel n. Here we are interested only in modes confined to the structure, and in general only over a certain frequency range, and so the integral range from $-\infty$ to ∞ is schematic; in general there will be mode cutoffs, and if the waveguide structure has periodicity in the z direction the range of k will at most be the first Brillouin zone. To take into account possible periodicity along the z direction of the structure we write

$$\mathbf{D}_{nIk}(\mathbf{r}) = \frac{\mathbf{d}_{nIk}(\mathbf{r})}{\sqrt{2\pi}} e^{ikz},$$
$$\mathbf{B}_{nIk}(\mathbf{r}) = \frac{\mathbf{b}_{nIk}(\mathbf{r})}{\sqrt{2\pi}} e^{ikz}, \tag{3}$$

where the functions $\mathbf{d}_{nIk}(\mathbf{r})$ and $\mathbf{b}_{nIk}(\mathbf{r})$ are periodic in the z direction with the periodicity, Λ_n, of the structure,

$$\mathbf{d}_{nIk}(\mathbf{r}) = \mathbf{d}_{nIk}(\mathbf{r} + \Lambda_n\hat{\mathbf{z}}),$$
$$\mathbf{b}_{nIk}(\mathbf{r}) = \mathbf{b}_{nIk}(\mathbf{r} + \Lambda_n\hat{\mathbf{z}}).$$

We assume no significant absorption or scattering losses in the frequency range of interest, but material dispersion is taken into account by determining $\mathbf{B}_{nIk}(\mathbf{r})$ and $\mathbf{D}_{nIk}(\mathbf{r})$, as previously discussed [29]; the solutions at k and $-k$ are not independent, and the relation between them can be fixed by taking

$$\mathbf{D}_{nI(-k)}(\mathbf{r}) = \mathbf{D}^*_{nIk}(\mathbf{r}),$$
$$\mathbf{B}_{nI(-k)}(\mathbf{r}) = -\mathbf{B}^*_{nIk}(\mathbf{r}). \tag{4}$$

We return to Fig. 2 now and look for solutions of the classical Maxwell equations for this structure that oscillate at frequency ω_{nIk} and have mode fields of the form

$$\mathbf{D}^{asy\text{-}in}_{nIk}(\mathbf{r}) = \mathbf{D}_{nIk}(\mathbf{r}_n) + \mathcal{D}^{out}_{nIk}(\mathbf{r}),$$
$$\mathbf{B}^{asy\text{-}in}_{nIk}(\mathbf{r}) = \mathbf{B}_{nIk}(\mathbf{r}_n) + \mathcal{B}^{out}_{nIk}(\mathbf{r}), \tag{5}$$

for positive k, where the *out* superscript indicates that far from the interaction region $\mathcal{D}^{out}_{nIk}(\mathbf{r})$ and $\mathcal{B}^{out}_{nIk}(\mathbf{r})$ consist of "outgoing" waves in each channel. That is, we have

$$\mathbf{D}^{asy\text{-}in}_{nIk}(\mathbf{r}) \sim \mathbf{D}_{nIk}(\mathbf{r}_n) + \sum_{n',I'\in\sigma_{n'}} \int_0^{\infty} dk'\, T^{out}_{nI;n'I'}(k,k')\mathbf{D}_{n'I'(-k')}(\mathbf{r}_{n'}), \tag{6}$$

for positive k. We refer to $(\mathbf{D}^{asy\text{-}in}_{nIk}(\mathbf{r}),\mathbf{B}^{asy\text{-}in}_{nIk}(\mathbf{r}))$ as an *asymptotic-in mode field*. In expressions like this when coordinates such as $\mathbf{r}_n$ appear on the right-hand side of the equation, the implication is that they should be evaluated at the physical point corresponding to the coordinates $\mathbf{r}$ in the laboratory frame appearing on the left-hand side of the equation [but recall (1)]. Since this mode field corresponds to a field oscillating at frequency ω_{nIk}, the only k' for which $T^{out}_{nI;n'I'}(k,k')$ can be nonvanishing are those for which $\omega_{n'I'k'} = \omega_{nIk}$ for positive k and k'. If we denote by $s_{nI;n'I'}(k)$ the positive value of k' for which indeed $\omega_{n'I'k'} = \omega_{nIk}$ holds for each given k, then $T^{out}_{nI;n'I'}(k,k')$ must be of the form

$$T^{out}_{nI;n'I'}(k,k') = \tau^{out}_{nI;n'I'}(k)\delta(k' - s_{nI;n'I'}(k)), \tag{7}$$

where the Dirac delta function provides the restriction.

The form of $\tau^{out}_{nI;n'I'}(k)$ is of course determined by the interaction region, but the physics of (6) is clear. Far from the interaction region, the exact solution $\mathbf{D}^{asy\text{-}in}_{nIk}(\mathbf{r})$ of Maxwell's equations corresponds to a wave *incoming* in mode I of channel n, and *outgoing* waves in general in all modes of all channels. Thus these asymptotic-in mode fields are analogous to the asymptotic-in states that appear in the elementary quantum theory of scattering [24]. They share with them an important feature, which we now recall.

Suppose that we construct a superposition of asymptotic-in mode fields of the form

$$\mathbf{D}(\mathbf{r},t) = \sum_{n,I\epsilon\sigma_n}\int_0^\infty dk\,\alpha_{nIk}e^{-i\omega_{nIk}t}\mathbf{D}^{asy\text{-}in}_{nIk}(\mathbf{r}) + \text{c.c.},$$
$$\mathbf{B}(\mathbf{r},t) = \sum_{n,I\epsilon\sigma_n}\int_0^\infty dk\,\alpha_{nIk}e^{-i\omega_{nIk}t}\mathbf{B}^{asy\text{-}in}_{nIk}(\mathbf{r}) + \text{c.c.} \tag{8}$$

We choose the complex amplitudes α_{nIk} such that, were we to put $\gamma_{nIk} = \alpha_{nIk}$ for $k > 0$ and vanishing otherwise in (2), we would have field profiles propagating in the $+z$ direction in each channel and, at $t = 0$, the field profiles would be centered at $z = 0$; at $t_0 \ll 0$, they would correspond to field profiles centered at $z \ll 0$. Following arguments in [24], as $t \to -\infty$ the fields $(\mathbf{D}(\mathbf{r},t), \mathbf{B}(\mathbf{r},t))$ of (8) can be written in the simplified form

$$\mathbf{D}(\mathbf{r},t) \to \sum_{n,I\epsilon\sigma_n}\int_0^\infty dk\,\alpha_{nIk}e^{-i\omega_{nIk}t}\mathbf{D}_{nIk}(\mathbf{r}_n) + \text{c.c.},$$
$$\mathbf{B}(\mathbf{r},t) \to \sum_{n,I\epsilon\sigma_n}\int_0^\infty dk\,\alpha_{nIk}e^{-i\omega_{nIk}t}\mathbf{B}_{nIk}(\mathbf{r}_n) + \text{c.c.} \tag{9}$$

That is, we have field profiles incident on the interaction region from the different channels; at such an early time the fields $\mathcal{D}^{out}_{nIk}(\mathbf{r})$ and $\mathcal{B}^{out}_{nIk}(\mathbf{r})$ in (5) can be neglected, not because they are small, but because they are added together with different phases in (8) for different k such that their net contribution vanishes. In practice one has to deal with systems that are characterized by channels of finite length. The results of (9) hold for channels that can be considered sufficiently long to contain the incoming pulse. As $t \to \infty$, on the other hand, when with our choice of γ_{nIk} in (2) the field profiles would be centered at $z \gg 0$, only the $\mathcal{D}^{out}_{nIk}(\mathbf{r})$ and $\mathcal{B}^{out}_{nIk}(\mathbf{r})$ in the asymptotic-in mode fields will make a contribution to (8). Indeed, the only regions of $\mathbf{r}_n$ for which the part of the field arising from the superposition of the $\mathbf{D}_{nIk}(\mathbf{r}_n)$ and $\mathbf{B}_{nIk}(\mathbf{r}_n)$ would make a contribution correspond to the region $D_n > z_n$ in the notation of (1), and thus do not correspond to regions in the physical structure. Thus for $t \to \infty$ there are only outgoing field profiles in each channel.

Such a superposition (8), with the amplitudes α_{nIk} properly chosen, corresponds to a scattering experiment with fields incident in general from each channel, as described by (9). Two important consequences follow from this. The first is that the asymptotic-in mode fields can be calculated numerically, even if they cannot be found or reasonably modeled analytically. The second is that, since the asymptotic-in mode fields can be used to model all scattering experiments, they can be used to describe all electromagnetic fields of the system, as long as there are no modes of the electromagnetic field completely bound to the interaction region. We plan to include such bound modes in treatments in later presentations, but here we assume they do not exist. And so (8) can be taken as an expansion of all electromagnetic fields of interest.

Similarly we can introduce asymptotic-out mode fields: they are full solutions of the Maxwell equations labeled by positive k and of the form

$$\mathbf{D}^{asy\text{-}out}_{nIk}(\mathbf{r}) = \mathbf{D}_{nI(-k)}(\mathbf{r}_n) + \mathcal{D}^{in}_{nIk}(\mathbf{r}),$$
$$\mathbf{B}^{asy\text{-}out}_{nIk}(\mathbf{r}) = \mathbf{D}_{nI(-k)}(\mathbf{r}_n) + \mathcal{B}^{in}_{nIk}(\mathbf{r}), \tag{10}$$

where the in superscript indicates that far from the interaction region $\mathcal{D}^{in}_{nIk}(\mathbf{r})$ and $\mathcal{B}^{in}_{nIk}(\mathbf{r})$ consist of incoming waves in each channel. That is,

$$\mathbf{D}^{asy\text{-}out}_{nIk}(\mathbf{r}) \sim \mathbf{D}_{nI(-k)}(\mathbf{r}_n) + \sum_{n',I'\in\sigma_{n'}}\int_0^\infty dk'\,T^{in}_{nI;n'I'}(k,k')\mathbf{D}_{n'I'k'}(\mathbf{r}_{n'}), \tag{11}$$

and, again using the fact that this field must be oscillating at frequency $\omega_{nI(-k)} = \omega_{nIk}$, the coefficient $T^{in}_{nI;n'I'}(k,k')$ must be of the form

$$T^{in}_{nI;n'I'}(k,k') = \tau^{in}_{nI;n'I'}(k)\delta(k' - s_{nI;n'I'}(k)).$$

We can identify the physics of these mode fields in analogy with the scenario considered above for the asymptotic-in mode fields. Here we construct

$$\mathbf{D}(\mathbf{r},t) = \sum_{n,I\epsilon\sigma_n}\int_0^\infty dk\,\beta_{nIk}e^{-i\omega_{nIk}t}\mathbf{D}^{asy\text{-}out}_{nIk}(\mathbf{r}) + \text{c.c.},$$
$$\mathbf{B}(\mathbf{r},t) = \sum_{n,I\epsilon\sigma_n}\int_0^\infty dk\,\beta_{nIk}e^{-i\omega_{nIk}t}\mathbf{B}^{asy\text{-}out}_{nIk}(\mathbf{r}) + \text{c.c.} \tag{12}$$

and now choose the complex amplitudes β_{nIk} such that, were we to put $\gamma_{nI(-k)} = \beta_{nIk}$ for $k > 0$ and vanishing otherwise in (2), we would have field profiles propagating in the $-z$ direction in each channel and, at $t = 0$, the field profiles would be centered at $z = 0$; at $t_1 \gg 0$, they would correspond to field profiles centered at $z \ll 0$. Again following arguments in [24], as $t \to \infty$ the fields $(\mathbf{D}(\mathbf{r},t), \mathbf{B}(\mathbf{r},t))$ of (12) can be written in the simplified form

$$\mathbf{D}(\mathbf{r},t) \to \sum_{n,I\epsilon\sigma_n}\int_0^\infty dk\,\beta_{nIk}e^{-i\omega_{nIk}t}\mathbf{D}_{nI(-k)}(\mathbf{r}_n) + \text{c.c.},$$
$$\mathbf{B}(\mathbf{r},t) \to \sum_{n,I\epsilon\sigma_n}\int_{-\infty}^\infty dk\,\beta_{nIk}e^{-i\omega_{nIk}t}\mathbf{B}_{nI(-k)}(\mathbf{r}_n) + \text{c.c.} \tag{13}$$

Here we have field profiles moving away from the interaction region in all the channels; as $t \to -\infty$, on the other hand, there are only incoming field profiles in each channel. Again, in the case of finite channels, (13) holds when they can be considered sufficiently long to contain the outgoing pulse.

Again neglecting any possible electromagnetic field modes bound to the interaction region, we can take (12) to be an expansion of all electromagnetic fields of interest. Indeed, both of the expansions (8) and (12) correspond to field profiles incident on the interaction region for $t \ll 0$ and field profiles moving away from the interaction region for $t \gg 0$. The difference is that in the asymptotic-in expansion it is easier to identify the amplitudes of the fields incident on the structure [the α_{nIk}; see (9)], and in the asymptotic-out expansion it is easier to identify the amplitudes of the fields departing from the structure [the β_{nIk}; see (13)]. Clearly the two sets of mode fields are not independent; comparing (6) and (11), and recalling the choice (4), we have

$$\begin{aligned}\mathbf{D}^{asy\text{-}out}_{nIk}(\mathbf{r}) &= \left[\mathbf{D}^{asy\text{-}in}_{nIk}(\mathbf{r})\right]^*,\\ \mathbf{B}^{asy\text{-}out}_{nIk}(\mathbf{r}) &= \left[-\mathbf{B}^{asy\text{-}in}_{nIk}(\mathbf{r})\right]^*.\end{aligned} \tag{14}$$

So a determination of the asymptotic-in mode fields suffices to determine the asymptotic-out mode fields as well. From the asymptotic forms (6) and (11) we find the relations

$$T^{in}_{nI;n'I'}(k,k') = \left[T^{out}_{nI;n'I'}(k,k')\right]^*. \tag{15}$$

These expressions allow us to rewrite a number of equations in the following section that involve the $T^{out}_{nI;n'I'}(k,k')$ in equivalent forms that instead involve the $T^{in}_{nI;n'I'}(k,k')$.

B. Quantum formulation

This is a convenient point to quantize the electromagnetic field. For the isolated channels of Fig. 3 we can write our field operators as

$$\begin{aligned}\mathbf{D}(\mathbf{r}) &= \sum_{n,I\epsilon\sigma_n}\int_{-\infty}^{\infty} dk\sqrt{\frac{\hbar\omega_{nIk}}{2}}c_{nIk}\mathbf{D}_{nIk}(\mathbf{r}) + \text{H.c.},\\ \mathbf{B}(\mathbf{r}) &= \sum_{n,I\epsilon\sigma_n}\int_{-\infty}^{\infty} dk\sqrt{\frac{\hbar\omega_{nIk}}{2}}c_{nIk}\mathbf{B}_{nIk}(\mathbf{r}) + \text{H.c.},\end{aligned} \tag{16}$$

where we work in the Schrödinger picture. The factors $\sqrt{\hbar\omega_{nIk}/2}$ are added for convenience and, for the mode fields $\mathbf{D}_{nIk}(\mathbf{r})$ and $\mathbf{B}_{nIk}(\mathbf{r})$ normalized properly [29], the operators c_{nIk} and their adjoints $c^\dagger_{nIk}$ satisfy the canonical commutation relations

$$\begin{aligned}[c_{nIk},c_{n'I'k'}] &= 0,\\ [c_{nIk},c^\dagger_{n'I'k'}] &= \delta_{nn'}\delta_{II'}\delta(k-k'),\end{aligned} \tag{17}$$

with the linear Hamiltonian for these isolated channels given by

$$H_{IC} = \sum_{n,I\epsilon\sigma_n}\int_{-\infty}^{\infty}\hbar\omega_{nIk}c^\dagger_{nIk}c_{nIk}, \tag{18}$$

neglecting the zero-point energy.

Turning now to the structure of Fig. 2, we will be interested in states $|\psi(t)\rangle$ such that for $t = t_0 \ll 0$ we have energy moving toward the interaction region, and for $t = t_1 \gg 0$ the energy will depart from the interaction region. We can expand the field operators in terms of the asymptotic-in fields,

$$\begin{aligned}\mathbf{D}(\mathbf{r}) &= \sum_{n,I\epsilon\sigma_n}\int_0^{\infty} dk\sqrt{\frac{\hbar\omega_{nIk}}{2}}a_{nIk}\mathbf{D}^{asy\text{-}in}_{nIk}(\mathbf{r}) + \text{H.c.},\\ \mathbf{B}(\mathbf{r}) &= \sum_{n,I\epsilon\sigma_n}\int_0^{\infty} dk\sqrt{\frac{\hbar\omega_{nIk}}{2}}a_{nIk}\mathbf{B}^{asy\text{-}in}_{nIk}(\mathbf{r}) + \text{H.c.},\end{aligned} \tag{19}$$

or asymptotic-out fields

$$\begin{aligned}\mathbf{D}(\mathbf{r}) &= \sum_{n,I\epsilon\sigma_n}\int_0^{\infty} dk\sqrt{\frac{\hbar\omega_{nIk}}{2}}b_{nIk}\mathbf{D}^{asy\text{-}out}_{nIk}(\mathbf{r}) + \text{H.c.},\\ \mathbf{B}(\mathbf{r}) &= \sum_{n,I\epsilon\sigma_n}\int_0^{\infty} dk\sqrt{\frac{\hbar\omega_{nIk}}{2}}b_{nIk}\mathbf{B}^{asy\text{-}out}_{nIk}(\mathbf{r}) + \text{H.c.}\end{aligned} \tag{20}$$

Looking at the first [Eq. (19)] of these, we use the expression (6) to write

$$\begin{aligned}\mathbf{D}(\mathbf{r}) \sim{}& \sum_{n,I\epsilon\sigma_n}\int_0^{\infty} dk\sqrt{\frac{\hbar\omega_{nIk}}{2}}a_{nIk}\mathbf{D}_{nIk}(\mathbf{r}_n) + \text{H.c.}\\ &+ \sum_{n,I\epsilon\sigma_n}\int_0^{\infty} dk\sqrt{\frac{\hbar\omega_{nIk}}{2}}\bar{c}_{nIk}\mathbf{D}_{nI(-k)}(\mathbf{r}_n) + \text{H.c.},\end{aligned} \tag{21}$$

where we have used (7) and

$$\bar{c}_{nIk} = \sum_{n',I'\epsilon\sigma_{n'}}\int_0^{\infty} a_{n'I'k'}T^{out}_{n'I';nI}(k',k)dk'. \tag{22}$$

Now as $t \to -\infty$ only the first term in (21) will be relevant, and since in this limit we could use either (21) or the isolated channel limit (16) to describe the electromagnetic field operators, following (17) we must have

$$\begin{aligned}[a_{nIk},a_{n'I'k'}] &= 0,\\ [a_{nIk},a^\dagger_{n'I'k'}] &= \delta_{nn'}\delta_{II'}\delta(k-k').\end{aligned} \tag{23}$$

As $t \to \infty$ only the second term in (21) will be relevant, and again since we could use either (21) or the isolated channel limit (16) we must have

$$\begin{aligned}[\bar{c}_{nIk},\bar{c}_{n'I'k'}] &= 0,\\ [\bar{c}_{nIk},\bar{c}^\dagger_{n'I'k'}] &= \delta_{nn'}\delta_{II'}\delta(k-k').\end{aligned} \tag{24}$$

The first of (24) automatically follows from (22), and the second identifies the condition

$$\begin{aligned}&\sum_{n',I'\epsilon\sigma_{n'}}\int dk'\ T^{out}_{n'I';n_1I_1}(k',k_1)\left[T^{out}_{n'I';n_2I_2}(k',k_2)\right]^*\\ &\quad = \delta_{n_1n_2}\delta_{I_1I_2}\delta(k_1-k_2).\end{aligned} \tag{25}$$

Corresponding arguments starting from (20) and the asymptotic form (11) of the asymptotic-out mode fields lead to

$$\begin{aligned}[b_{nIk},b_{n'I'k'}] &= 0,\\ [b_{nIk},b^\dagger_{n'I'k'}] &= \delta_{nn'}\delta_{II'}\delta(k-k'),\end{aligned} \tag{26}$$

and again (25), written in terms of the $T^{in}_{n'I';nI}(k',k)$ [recall (15)].

We can now identify the relation between the $\mathbf{D}^{asy\text{-}out}_{nIk}(\mathbf{r})$ and the $\mathbf{D}^{asy\text{-}in}_{nIk}(\mathbf{r})$; (14) gives one relation involving complex conjugation, but since both asymptotic-in and -out fields are complete it is possible to identify a relation of the form

$$\mathbf{D}^{asy\text{-}out}_{nIk}(\mathbf{r}) = \sum_{n',I'\epsilon\sigma_{n'}}\int dk'\ \mathcal{C}(nIk;n'I'k')\mathbf{D}^{asy\text{-}in}_{n'I'k'}(\mathbf{r}). \tag{27}$$

As both $\mathbf{D}_{nIk}^{asy\text{-}out}(\mathbf{r})$ and $\mathbf{D}_{nIk}^{asy\text{-}in}(\mathbf{r})$ correspond to solutions with frequency ω_{nIk}, we can expect the coefficients $\mathcal{C}(nIk;n'I'k')$ to contain a factor $\delta(k'-s_{nI;n'I'}(k))$. It suffices to look at the asymptotic form of the two sides of (14) and compare the outgoing parts; these must be equal, and using (6) and (11) we find this is satisfied with $\mathcal{C}(nIk;n'I'k')=[T_{n'I';nI}^{out}(k',k)]^*=T_{n'I';nI}^{in}(k',k)$, where we have used (15). So we have

$$\mathbf{D}_{nIk}^{asy\text{-}out}(\mathbf{r})=\sum_{n',I'\epsilon\sigma_{n'}}\int dk'\ T_{n'I';nI}^{in}(k',k)\mathbf{D}_{n'I'k'}^{asy\text{-}in}(\mathbf{r}). \quad (28)$$

The factor $T_{n'I';nI}^{in}(k',k)$ is restricted to $k=s_{n'I';nI}(k')$, which is the same as the restriction $k'=s_{nI;n'I'}(k)$ that was expected. With this in hand, we can determine the relation between the lowering operators a_{nIk} and b_{nIk} appearing in the expansions (19) and (20) in terms of asymptotic-in and asymptotic-out fields, respectively. Using (28) in (20) and comparing with (19), we find

$$a_{nIk}=\sum_{n',I'\epsilon\sigma_{n'}}\int_0^\infty dk' T_{nI;n'I'}^{in}(k,k')b_{n'I'k'}. \quad (29)$$

Using the commutation relations for the a_{nIk} and their adjoints (23), and those of the b_{nIk} and their adjoints (26), along with (15), we find

$$\sum_{n',I'\epsilon\sigma_{n'}}\int dk'\ T_{n_1I_1;n'I'}^{out}(k_1,k')\big[T_{n_2I_2;n'I'}^{out}(k_2,k')\big]^* = \delta_{n_1n_2}\delta_{I_1I_2}\delta(k_1-k_2), \quad (30)$$

which complements (25). Expressions for $\mathbf{D}_{nIk}^{asy\text{-}in}(\mathbf{r})$ in terms of the $\mathbf{D}_{nIk}^{asy\text{-}out}(\mathbf{r})$, and the b_{nIk} in terms of the a_{nIk}, can be similarly derived; we find

$$\mathbf{D}_{nIk}^{asy\text{-}in}(\mathbf{r})=\sum_{n',I'\epsilon\sigma_{n'}}\int dk'\ T_{n'I';nI}^{out}(k',k)\mathbf{D}_{n'I'k'}^{asy\text{-}out}(\mathbf{r}) \quad (31)$$

and

$$b_{nIk}=\sum_{n',I'\epsilon\sigma_{n'}}\int_0^\infty dk'\ T_{nI;n'I'}^{out}(k,k')a_{n'I'k'}. \quad (32)$$

C. Scattering in the linear regime

We now treat the quantum optics of scattering from our structure in the linear regime. Because of the form of the isolated channel Hamiltonian, arguments along the lines of those following (19) and (20) lead to a Hamiltonian for the structure of Fig. 2 of

$$H_L=\sum_{n,I\epsilon\sigma_n}\int_0^\infty dk\,\hbar\omega_{nIk}a_{nIk}^\dagger a_{nIk} = \sum_{n,I\epsilon\sigma_n}\int_0^\infty dk\,\hbar\omega_{nIk}b_{nIk}^\dagger b_{nIk}.$$

We construct an initial state $|\psi(t_0)\rangle$ for $t_0\ll 0$ that corresponds to energy incident on the interaction region from one or more of the channels. We write this state in the form

$$|\psi(t_0)\rangle = e^{-iH_Lt_0/\hbar}K_{in}(\{a_{nIk}\},\{a_{nIk}^\dagger\})|\text{vac}\rangle = K_{in}(\{a_{nIk}e^{i\omega_{nIk}t_0}\},\{a_{nIk}^\dagger e^{-i\omega_{nIk}t_0}\})|\text{vac}\rangle, \quad (33)$$

where $|\text{vac}\rangle$ is the vacuum state of the system, $K_{in}(\{a_{nIk}\},\{a_{nIk}^\dagger\})$ is a function of the sets of operators indicated, and in the second line we have used the fact that $\exp(-iH_Lt_0/\hbar)|\text{vac}\rangle=|\text{vac}\rangle$. Because of the nature of the asymptotic-in mode fields, it will be easy to write down expectation values of operators in $|\psi(t_0)\rangle$, as we illustrate in an example below. Note that at all later times we will have

$$|\psi(t)\rangle = e^{-iH_Lt/\hbar}K_{in}(\{a_{nIk}\},\{a_{nIk}^\dagger\})|\text{vac}\rangle. \quad (34)$$

For times $t\gg 0$, however, it will be convenient to write the set $\{a_{nIk}\}$ in terms of the set $\{b_{nIk}\}$, and the set $\{a_{nIk}^\dagger\}$ in terms of the set $\{b_{nIk}^\dagger\}$, using (29). The function $K_{in}(\{a_{nIk}\},\{a_{nIk}^\dagger\})$ written in terms of the $\{b_{nIk}\}$ and $\{b_{nIk}^\dagger\}$ will then define a new function according to

$$K_{out}(\{b_{nIk}\},\{b_{nIk}^\dagger\})=K_{in}(\{a_{nIk}\},\{a_{nIk}^\dagger\}),$$

where the use of (29) is implicit. At any time, from (33) we can then write

$$|\psi(t)\rangle = e^{-iH_Lt/\hbar}K_{out}(\{b_{nIk}\},\{b_{nIk}^\dagger\})|\text{vac}\rangle,$$

and so at a time $t_1\gg 0$ we then have

$$|\psi(t_1)\rangle = e^{-iH_Lt_1/\hbar}K_{out}(\{b_{nIk}\},\{b_{nIk}^\dagger\})|\text{vac}\rangle = K_{out}(\{b_{nIk}e^{i\omega_{nIk}t_1}\},\{b_{nIk}^\dagger e^{-i\omega_{nIk}t_1}\})|\text{vac}\rangle, \quad (35)$$

and due to the properties of the asymptotic-out mode fields it will be convenient to write down the expectation values of operators at t_1 using this form.

As an example, suppose we want to describe coherent states incident on the structure at t_0. Then we take

$$K_{in}(\{a_{nIk}\},\{a_{nIk}^\dagger\})=e^{\Gamma_{in}(\{a_{nIk}\},\{a_{nIk}^\dagger\};0)},$$

where

$$\Gamma_{in}(\{a_{nIk}\},\{a_{nIk}^\dagger\};t) = \sum_{n,I\epsilon\sigma_n}\int_0^\infty dk\ \nu_{nIk}e^{-i\omega_{nIk}t}a_{nIk}^\dagger - \text{H.c.}$$

and the ν_{nIk} are complex numbers; from (33) we have

$$|\psi(t_0)\rangle = e^{\Gamma_{in}(\{a_{nIk}\},\{a_{nIk}^\dagger\};t_0)}|\text{vac}\rangle.$$

In evaluating $\langle\psi(t_0)|\mathbf{D}(\mathbf{r})|\psi(t_0)\rangle$ we will have

$$\langle\psi(t_0)|\mathbf{D}(\mathbf{r})|\psi(t_0)\rangle \to \sum_{n,I\epsilon\sigma_n}\int_0^\infty dk\sqrt{\frac{\hbar\omega_{nIk}}{2}}\nu_{nIk}e^{-i\omega_{nIk}t_0}\mathbf{D}_{nIk}(\mathbf{r})+\text{c.c.},$$

$$t_0\ll 0,$$

which mimics our classical description [see the first of (9)], assuming that the $\nu_{nIk}\sqrt{\hbar\omega_{nIk}/2}$ have the properties of α_{nIk}; only the incoming part makes a contribution to the asymptotic-in field expansion of (21). Now using (29) and (15) we can construct $K_{out}(\{b_{nIk}\},\{b_{nIk}^\dagger\})$; we find

$$K_{out}(\{b_{nIk}\},\{b_{nIk}^\dagger\})=e^{\Gamma_{out}(\{b_{nIk}\},\{b_{nIk}^\dagger\};0)},$$

where

$$\Gamma_{out}(\{b_{nIk}\},\{b_{nIk}^{\dagger}\};t) = \sum_{n,I\epsilon\sigma_n}\int_0^{\infty}dk\left[\sum_{n',I'\epsilon\sigma_{n'}}\int_0^{\infty}dk' T^{out}_{n'I';nI}(k',k)\nu_{n'I'k'}\right] \times e^{-i\omega_{nIk}t}b_{nIk}^{\dagger} - \text{H.c.}$$

Then from (35) we have

$$|\psi(t_1)\rangle = e^{\Gamma_{out}(\{b_{nIk}\},\{b_{nIk}^{\dagger}\};t_1)}|\text{vac}\rangle,$$

and for t_1 large enough only the outgoing part of $\mathbf{D}^{asy\text{-}out}_{nIk}(\mathbf{r})$ [see (11)] in the first of (20) will give a contribution to quantities such as $\langle\psi(t_1)|\mathbf{D}(\mathbf{r})|\psi(t_1)\rangle$, and we will have

$$\langle\psi(t_1)|\mathbf{D}(\mathbf{r})|\psi(t_1)\rangle \to \sum_{n,I\epsilon\sigma_n}\int_0^{\infty}dk\sqrt{\frac{\hbar\omega_{nIk}}{2}} \times\left[\sum_{n',I'\epsilon\sigma_{n'}}\int_0^{\infty}dk'\, T^{out}_{n'I';nI}(k',k)\nu_{n'I'k'}\right] \times e^{-i\omega_{nIk}t_1}\mathbf{D}_{nI(-k)}(\mathbf{r}_n) + \text{c.c.},\quad t_1 \gg 0. \tag{36}$$

This example is particularly simple because it essentially repeats the classical calculation given earlier. Indeed, following the calculation (9) to times $t \gg 0$ and using the results of the discussion below that equation, we find the same expression as (36) if we replace $\nu_{nIk}\sqrt{\hbar\omega_{nIk}/2}$ by α_{nIk}. More important is the general strategy, which allows us to move from a representation in terms of the asymptotic-in mode fields to one in terms of the asymptotic-out mode fields and can be applied to more general states of the electromagnetic field. In the simple linear case here the scattering is described by nothing more than that change of basis; the physics of the scattering is contained within the asymptotic mode fields themselves. If nonlinearities are included the situation is more complicated, but the strategy devised here can be extended to aid in the solution of such problems. We turn to that in the next section.

IV. SCATTERING WITH NONLINEARITIES

We now include a nonlinear term in our Hamiltonian,

$$H = H_L + H_{NL},$$

assuming that only field operators in the interaction region contribute to H_{NL}. We can then still start with a state $|\psi(t_0)\rangle$ at $t_0 \ll 0$ consisting of energy incident on the interaction region but far from it, because there is no nonlinearity in the region of excitation,

$$|\psi(t_0)\rangle = e^{-iH_Lt_0/\hbar}K_{in}(\{a_{nIk}\},\{a_{nIk}^{\dagger}\})|\text{vac}\rangle.$$

We now define an *asymptotic-in ket* $|\psi_{in}\rangle$ as the ket to which this would evolve at $t = 0$ were there no nonlinearity:

$$|\psi_{in}\rangle = e^{-iH_L(0-t_0)/\hbar}|\psi(t_0)\rangle = K_{in}(\{a_{nIk}\},\{a_{nIk}^{\dagger}\})|\text{vac}\rangle. \tag{37}$$

In fact the ket evolves according to the entire Hamiltonian H, and at a later time t_1 the ket will be

$$|\psi(t_1)\rangle = e^{-iH(t_1-t_0)/\hbar}|\psi(t_0)\rangle.$$

The *asymptotic-out ket* is the ket that would evolve to this from $t = 0$ were there no nonlinearity,

$$|\psi(t_1)\rangle = e^{-iH_L(t_1-0)/\hbar}|\psi_{out}\rangle, \tag{38}$$

or

$$|\psi_{out}\rangle = e^{iH_Lt_1/\hbar}|\psi(t_1)\rangle = e^{iH_Lt_1/\hbar}e^{-iH(t_1-t_0)/\hbar}|\psi(t_0)\rangle = e^{iH_Lt_1/\hbar}e^{-iH(t_1-t_0)/\hbar}e^{-iH_Lt_0/\hbar}|\psi_{in}\rangle = U(t_1,t_0)|\psi_{in}\rangle,$$

where

$$U(t_1,t_0) \equiv e^{iH_Lt_1/\hbar}e^{-iH(t_1-t_0)/\hbar}e^{-iH_Lt_0/\hbar}. \tag{39}$$

The entire effect of the nonlinearity is described in the transition $|\psi_{in}\rangle \to |\psi_{out}\rangle$; the rest of the dynamics in the evolution from $|\psi(t_0)\rangle \to |\psi(t_1)\rangle$ is purely linear and more easily described. In the absence of nonlinearity, of course, $H = H_L$ and clearly $|\psi_{out}\rangle = |\psi_{in}\rangle$. More generally, although the form (37) is the easiest in which to specify the incoming fields, for the ultimate calculation of the outgoing fields it is usually more convenient to use the alternative form

$$|\psi_{in}\rangle = K_{out}(\{b_{nIk}\},\{b_{nIk}^{\dagger}\})|\text{vac}\rangle.$$

Then the transition to $|\psi_{out}\rangle$,

$$|\psi_{out}\rangle = U(t_1,t_0)K_{out}(\{b_{nIk}\},\{b_{nIk}^{\dagger}\})|\text{vac}\rangle$$

can be calculated or approximated using the asymptotic-out basis, as well as, if desired, the transformation (38) to $|\psi(t_1)\rangle$. However, we will see that this general strategy can be simplified in examples we give below.

We now turn to the specific form of the nonlinear Hamiltonian, which in our approach should be written in terms of the asymptotic fields. With the neglect of any nonlinear magneto-optical effects, and ignoring material dispersion in the *nonlinear* response of the medium, the nonlinear Hamiltonian H_{LN} that should be added to H_L to construct the full Hamiltonian in the Schrödinger picture is

$$H_{NL} = -\frac{1}{3\varepsilon_0}\int d\mathbf{r}\,\Gamma_2^{ijk}(\mathbf{r})D^i(\mathbf{r})D^j(\mathbf{r})D^k(\mathbf{r}) - \frac{1}{4\varepsilon_0}\int d\mathbf{r}\,\Gamma_3^{ijkl}(\mathbf{r})D^i(\mathbf{r})D^j(\mathbf{r})D^k(\mathbf{r})D^l(\mathbf{r}) + \cdots, \tag{40}$$

where the superscripts indicate Cartesian coordinates and are to be summed over when repeated, and the $\Gamma_n(\mathbf{r})$ are nth-rank tensors that are symmetric under the permutations of all indices [30]. In the specific quantum examples we present, we consider SPDC in which a pump photon, coming through channel m, is converted into two photons in the interaction region that exit through channel n. A natural choice is to write the field operators associated with channel m in terms of the asymptotic-in fields and those associated with channel n in terms of asymptotic-out fields. Thus, assuming single-mode channels for simplicity, so that we can neglect the index I

in our notation, the relevant (energy-conserving) term in the nonlinear Hamiltonian is

$$H_{NL} = -\int dk_1 dk_2 dk S_{nn;m}(k_1,k_2,k) b^{\dagger}_{nk_1} b^{\dagger}_{nk_2} a_{mk} + \text{H.c.}, \tag{41}$$

where

$$S_{nn;m}(k_1,k_2,k) = \frac{1}{\varepsilon_0}\sqrt{\frac{(\hbar\omega_{nk_1})(\hbar\omega_{nk_2})(\hbar\omega_{mk})}{8}} \int d\mathbf{r}\, \Gamma_2^{ijk}(\mathbf{r}) \times \left[D^{i,asy\text{-}out}_{nk_1}(\mathbf{r})\right]^* \left[D^{j,asy\text{-}out}_{nk_2}\right]^*(\mathbf{r}) D^{k,asy\text{-}in}_{mk}(\mathbf{r}), \tag{42}$$

and we have used (19) and (20). Of course, we could use (14) or (31) along with (29) to rewrite the above expression entirely in terms of asymptotic-out fields and operators, but the form above is most illustrative of the physics.

Conventionally the second-order response is specified not by $\Gamma_2^{ijk}(\mathbf{r})$, which relates the nonlinear polarization to the displacement field, but by $\varepsilon_0\chi_2^{ijk}(\mathbf{r})$, which relates the nonlinear polarization to the electric fields. As discussed earlier [30], if the material dispersion is neglected in $\chi_2^{ijk}(\mathbf{r})$ then in (42) we should take

$$\Gamma_2^{ijk}(\mathbf{r}) \to \frac{\chi_2^{ijk}(\mathbf{r})}{\varepsilon_0 n^2(\mathbf{r},\omega_{nk_1}) n^2(\mathbf{r},\omega_{nk_2}) n^2(\mathbf{r},\omega_{mk})}, \tag{43}$$

where $n(\mathbf{r},\omega)$ is the material refractive index at position $\mathbf{r}$ and frequency ω.

V. EXAMPLE I: SPDC IN MICRORING RESONATORS

In this section the photonic system considered is a microring resonator such as the one sketched in Fig. 4. Microring resonators are attractive as photon pair sources because they can be integrated with silicon technologies [31–33], can achieve quasi-phase-matching at frequencies far from degeneracy without the need for complicated dispersion engineering [34], and are predicted to generate frequency-anticorrelated or -uncorrelated photon pairs by simply varying the pump pulse duration [17,18]; photon pair generation in a microring resonator has already been observed [16].

The specific system that we study is a GaAs microring resonator (see Fig. 4), grown with $\hat{\mathbf{y}}$ corresponding to a crystal axis, and side-coupled to a channel waveguide at a single point, $z = 0$. Although the formalism can be applied to more complex

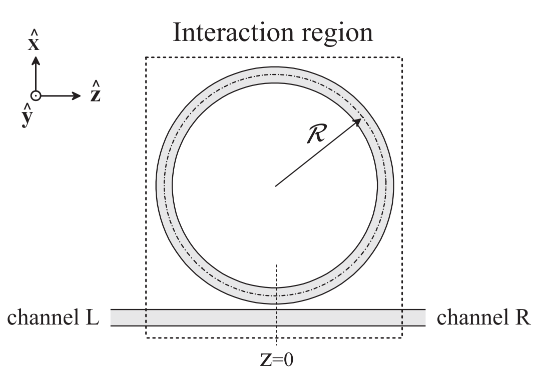

FIG. 4. Sketch of the ring resonator.

systems and take into account coupling more realistic than that taken to occur at a single point, we consider this simple model studied earlier [15] to demonstrate the simplicity with which previous results can be recovered. We assume pump photons coming from the left [$m = L$ in (41)] and generated photons exiting on the right side of the ring [$n = R$ in (41)].

We construct a full solution for one of the $D^{i,asy\text{-}in}_{Lk}(\mathbf{r})$ according to

$$D^{i,asy\text{-}in}_{Lk}(\mathbf{r}) = \begin{cases} \frac{d^i_k(\mathbf{r}_\perp)}{\sqrt{2\pi}} e^{ikz} \text{ when } z < 0, \\ T(k)\frac{d^i_k(\mathbf{r}_\perp)}{\sqrt{2\pi}} e^{ikz} \text{ when } z > 0, \\ +D^{i,ring}_{Lk}(\mathbf{r}) \text{ in the ring,} \end{cases} \tag{44}$$

where $\mathbf{r}_\perp$ indicates the coordinates in the plane normal to the waveguide (whether in a channel or in the ring), and treat the coupling between the channels and the ring in the usual way, with self-, $\sigma(k)$, and cross-, $\kappa(k)$, coupling coefficients satisfying $\sigma(k)^2 + \kappa(k)^2 = 1$, and where

$$|T(k)|^2 = |\sigma(k) + \frac{[i\kappa(k)]^2 e^{ik\ell}}{1-\sigma(k)e^{ik\ell}}|^2 = 1 \tag{45}$$

if losses are neglected. Note that the mode profiles $d^i_k(\mathbf{r}_\perp)$ are not labeled by a channel index (L or R), as they are identical in both channels here, whereas the $D^{i,ring}_{Lk}(\mathbf{r})$ are, as a field incident from the left channel will propagate counterclockwise around the ring compared to a field incident from the right channel which will propagate clockwise, i.e.,

$$D^{i,ring}_{Lk}(\mathbf{r}) = \frac{i\kappa(k)}{1-\sigma(k)e^{ik\ell}} \frac{d^i_k(\mathbf{r}_\perp,\zeta/R)}{\sqrt{2\pi}} e^{ik\zeta}, \tag{46}$$

where ζ is the coordinate in the counterclockwise direction along the ring circumference of length $\ell = 2\pi R$. A similar construction follows for the $[D^{i,asy\text{-}out}_{Rk}(\mathbf{r})]^*$.

Note that, in a GaAs microring, fields polarized in the plane of the ring (x polarized in the channel) experience a change in local coordinates with respect to the crystal coordinates, and thus a change in nonlinearity, as they travel around the ring. Rather than have the ring mode profiles depend explicitly on ζ/R, we consider rotation matrices that connect components along the circumference of the ring, $d^i_k(\mathbf{r}_\perp,\zeta/R)$, to their corresponding channel components, $d^i_k(\mathbf{r}_\perp)$, and allow us to pull this dependence out of integrals over $\mathbf{r}_\perp$. Recalling that in GaAs there is only one independent component of χ_2^{ijk}, i.e., that all components for which $i \neq j \neq k$ are equal, and calling it $\overline{\chi}_2$, for a pump polarized perpendicular to the plane of the ring (y polarized in the channel) these considerations lead to both down-converted fields being x polarized in the channel, and allow us to write the nonlinear coupling term (41) as

$$S_{RR;L}(k_1,k_2,k) = \sqrt{\frac{(\hbar\omega_{k_1})(\hbar\omega_{k_2})(\hbar\omega_k)}{(4\pi)^3\varepsilon_0}} \frac{\overline{\chi}_2}{\overline{n}^3} I \frac{i\kappa(k_1)}{1-\sigma(k_1)e^{ik_1\ell}} \times \frac{i\kappa(k_2)}{1-\sigma(k_2)e^{ik_2\ell}} \frac{i\kappa(k)}{1-\sigma(k)e^{ik\ell}} \frac{e^{i\phi(k_1,k_2,k)}}{\sqrt{\mathcal{A}(k_1,k_2,k)}}, \tag{47}$$

where

$$\frac{e^{i\phi(k_1,k_2,k)}}{\sqrt{\mathcal{A}(k_1,k_2,k)}} = 2\int d\mathbf{r}_\perp \frac{\overline{n}^3 d^y_{k_1}(\mathbf{r}_\perp)d^y_{k_2}(\mathbf{r}_\perp)d^x_k(\mathbf{r}_\perp)}{\varepsilon_0^{3/2} n^2(\mathbf{r}_\perp;\omega_{k_1})n^2(\mathbf{r}_\perp;\omega_{k_2})n^2(\mathbf{r}_\perp;\omega_k)}, \quad (48)$$

with the integral taken over the channel cross section defining the effective area $\mathcal{A}(k_1,k_2,k)$. We have dropped all redundant channel labels, $\overline{n}$ is a reference refractive index introduced solely for convenience, and

$$\begin{aligned} I &= \int_0^\ell d\zeta e^{i\Delta k\zeta}\cos(\zeta/R)\sin(\zeta/R) \\ &= \frac{e^{i\pi(\Delta kR+2)}}{4i}\frac{\ell\sin[\pi(\Delta kR+2)]}{\pi(\Delta kR+2)} \\ &\quad -\frac{e^{i\pi(\Delta kR-2)}}{4i}\frac{\ell\sin[\pi(\Delta kR-2)]}{\pi(\Delta kR-2)} \end{aligned} \quad (49)$$

identifies the quasi-phase-matching condition $\Delta k(= k - k_1 - k_2) = \pm 2/R$. We have also assumed that the structure is dispersion engineered such that pump and down-converted fields are all near ring resonances, so the nonlinear interaction in the ring dominates that in the channel and the latter can be neglected. With these expressions in hand we can apply the backward Heisenberg picture approach, as outlined in [35] to calculate the state of generated photons in the undepleted pump approximation, characterized by the biphoton wave function (BWF)

$$\begin{aligned} &\widetilde{\phi}_{RR;L}(\omega_1,\omega_2) \\ &= \frac{2\sqrt{2}\pi\alpha}{\beta}\frac{i}{\hbar}\frac{1}{\sqrt{v_g(\omega_1)v_g(\omega_2)v_g(\omega_1+\omega_2)}}\widetilde{\phi}_P(\omega_1+\omega_2) \\ &\quad \times S_{RR;L}(k(\omega_1),k(\omega_2),k(\omega_1+\omega_2)), \end{aligned} \quad (50)$$

where the $v_g(\omega)$ are group velocities, and $\widetilde{\phi}_P(\omega)$ is the pump pulse wave form containing, on average, $|\alpha|^2$ photons. Note that the BWF and pump wave form are normalized with respect to frequency rather than wave vector, the former by setting the value of the normalization constant β; the relation between these functions in frequency space and momentum space was discussed earlier [35] and is mentioned in the Appendix. In the limit of a small probability of pair production per pump pulse, that probability is given by

$$\begin{aligned} |\beta|^2 &= \frac{\hbar|\alpha|^2(\overline{\chi}_2)^2}{8\pi\varepsilon_0 v^2_{g_F} v_{g_S}\mathcal{A}\overline{n}^6} \\ &\quad \times \int_0^\infty d\omega_1 d\omega_2 |\widetilde{\phi}_P(\omega_1+\omega_2)|^2\omega_1\omega_2(\omega_1+\omega_2) \\ &\quad \times \left| I\frac{i\kappa_F}{1-\sigma_F e^{ik(\omega_1)\ell}}\frac{i\kappa_F}{1-\sigma_F e^{ik(\omega_2)\ell}}\frac{i\kappa_S}{1-\sigma_S e^{ik(\omega_1+\omega_2)\ell}}\right|^2. \end{aligned} \quad (51)$$

Although the coupling coefficients and group velocities truly have some frequency dependence, here we have taken them as constant for wave vectors associated with second harmonic frequencies (i.e., for terms involving $\omega_1+\omega_2$ over the bandwidth of the pump) and labeled by S, and also constant for wave vectors associated with down-converted, fundamental, frequencies (i.e., for terms involving just ω_1 or ω_2 over the SPDC bandwidth) and labeled by F. We have also taken $\mathcal{A}(k(\omega_1),k(\omega_2),k(\omega)) = \mathcal{A}$ to be essentially constant over the frequency range of interest and thus pulled it out of the integral. We stress how similar these expressions (50) and (51) are to the detailed example in [35], and also that no additional ring or coupling Hamiltonians, along with their associated subtleties, were required. We now proceed to perform the integrals over ω_1 and ω_2 and calculate $|\beta|^2$ explicitly, to show that the new formalism reproduces the previous result.

We work in the limit of a long pulse, narrowly centered at resonance frequency ω_S such that $|\widetilde{\phi}_P(\omega_1+\omega_2)|^2 \approx \delta(\omega_1+\omega_2-\omega_S)$ and, as mentioned above, assume that the ring has been dispersion engineered such that the pump field at ω_S as well as the down-converted fields at frequencies on either side of half the pump, $\omega_{F^\pm} = \omega_S/2 \pm \Delta\omega$, are exactly on the resonances centered in k space at k_{S_0} and $k_{F^\pm} = (k_{S_0}/2 - 1/R) \pm 1/R$, respectively. Then, expanding the wave vectors to first order around k_{S_0} and $k_{F^\pm}$, we may make the Lorentzian approximation for the field coupling terms, e.g., $|i\kappa_F/\{1-\sigma_F\exp[ik_F(\omega_{1(2)})\ell]\}|^2 \approx \kappa_F^2/\{\ (1-\sigma_F)^2 + [(\omega - \omega_{F^{+(-)}})\ell/v_{g_F}]^2\}$ and extend the range of integration over ω_1 and ω_2 from $-\infty$ to ∞. Thus, we no longer consider the total probability of generating a photon pair within any pair of resonance linewidths, but rather, for a pump centered at resonance frequency ω_S, focus our attention on the pairs of photons generated within the linewidths defined by $k_{F^\pm}$. Calling this new quantity $|\beta_{F^\pm}|^2$ and integrating over ω_2, we find

$$\begin{aligned} \frac{|\beta_{F^\pm}|^2}{|\alpha|^2} &\approx 2\frac{\hbar(\overline{\chi}_2)^2\omega_S}{8\pi\varepsilon_0 v^2_{g_F} v_{g_S}\mathcal{A}\overline{n}^6}\frac{\kappa_S^2}{(1-\sigma_S)^2}\int_{-\infty}^\infty d\omega_1\omega_1(\omega_S-\omega_1) \\ &\quad \times |I|^2\frac{\kappa_F^4}{((1-\sigma_F)^2+\{\sigma_F[\omega_1-(\omega_S/2+\Delta\omega)]\ell/v_{g_F}\}^2)^2}. \end{aligned}$$

These assumptions have the additional implication that the quasi-phase-matched sinc function resulting from the integral I is essentially unity, i.e., for the particular ring design and resonances considered, only the second term in (49) is appreciable, and approximately equal to $i\ell/4$. Making the change of variables $\Omega = \sigma_F[\omega_1 - (\omega_S/2+\Delta\omega)]\ell/v_{g_F}$ and keeping only the term proportional to ω_S^2, by far the largest, we find

$$\begin{aligned} \frac{|\beta_{F^\pm}|^2}{|\alpha|^2} &\approx \frac{\hbar(\overline{\chi}_2)^2\ell\omega_S^3}{256\pi\varepsilon_0 v^2_{g_F} v_{g_S}\mathcal{A}\overline{n}^6\sigma_F}\frac{\kappa_S^2}{(1-\sigma_S)^2} \\ &\quad \times \int_{-\infty}^\infty d\Omega\frac{\kappa_F^4}{[(1-\sigma_F)^2+\Omega^2]^2} \\ &= \frac{\hbar(\overline{\chi}_2)^2\ell\omega_S^3}{512\varepsilon_0 v_{g_F} v_{g_S}\mathcal{A}\overline{n}^6\sigma_F}\frac{\kappa_F^2}{(1-\sigma_F)^2}\frac{\kappa_S^4}{(1-\sigma_S)^3}. \end{aligned}$$

If we then introduce

$$\mathcal{P} = \frac{8\varepsilon_0\overline{n}^6 v^2_{g_F} v_{g_S}}{(\overline{\chi}_2)^2\omega_S^2},$$

$$P_F = \frac{\hbar\omega_S v_{g_F}}{2\ell},$$

and make the usual assumptions that $\sigma_F \approx 1, \sigma_S \approx 1$, we arrive at our final expression

$$\frac{|\beta_{F^\pm}|^2}{|\alpha|^2} = \frac{P_F}{\mathcal{P}} \frac{\ell^2}{\mathcal{A}} \frac{1}{16} \alpha_F^2 \alpha_S^2, \tag{52}$$

where

$$\alpha_m^2 = \frac{2}{1-\sigma_m},$$

exactly as in [15].

VI. EXAMPLE II: SECOND HARMONIC GENERATION AND SPDC IN LAYERED STRUCTURES

In this section we apply the strategy of asymptotic fields to the description of SHG and SPDC in planar one-dimensional photonic crystal structures such as the one shown in Fig. 5. This choice is motivated by two reasons: (i) Historically, SHG has been widely studied in periodic multilayers [36–46], as they are very simple structures with respect to both fabrication and theoretical description. A number of designs to enhance the effect of the nonlinearity have been suggested, and many of them are now potentially interesting for SPDC enhancement. (ii) We want to stress that our approach is not limited to the case of integrated photonic circuits, where light is coupled in and out of the photonic system through waveguides, but it is much more general and can be used to describe several experimental configurations.

First we focus on SHG: Two pump photons coming from the right channel are converted into a photon exiting the left channel (see Fig. 5), a scenario opposite to that considered in the previous section. Starting from (40), we extract the relevant term in the nonlinear Hamiltonian

$$H_{NL} = -\int dk dk_1 dk_2 S_{L;RR}(k,k_1,k_2) b_{Lk}^\dagger a_{Rk_1} a_{Rk_2} + \text{H.c.}, \tag{53}$$

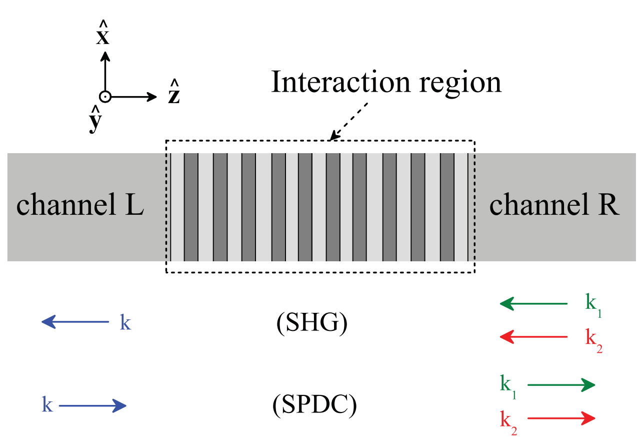

FIG. 5. (Color online) Sketch of a one-dimensional photonic crystal.

with nonlinear coupling parameter

$$S_{L;RR}(k,k_1,k_2) = \frac{1}{\varepsilon_0}\sqrt{\frac{(\hbar\omega_{Lk})(\hbar\omega_{Rk_1})(\hbar\omega_{Rk_2})}{8}} \times \int d\mathbf{r}\, \Gamma_2^{ijk}(\mathbf{r})[D_{Lk}^{i,asy\text{-}out}(\mathbf{r})]^* D_{Rk_1}^{j,asy\text{-}in}(\mathbf{r}) D_{Rk_2}^{k,asy\text{-}in}(\mathbf{r}), \tag{54}$$

in analogy with (41) and (42) above.

In the case of the multilayer of interest (see Fig. 5), the channels are the semiinfinite layers on each side of the structure, and the electromagnetic field is described in terms of plane waves. If we consider a linearly polarized plane wave of frequency ω propagating in the right channel in the $-\hat{\mathbf{z}}$ direction, the displacement field can be written

$$\mathbf{D}_{Rk}(\mathbf{r}) = \hat{\mathbf{e}}\sqrt{\frac{\epsilon_0 n_R^2(\omega_{Rk})}{2\pi A}\frac{v_{gR}(\omega_{Rk})}{v_{pR}(\omega_{Rk})}}e^{-ikz}, \tag{55}$$

where $\hat{\mathbf{e}}$ is perpendicular to $\hat{\mathbf{z}}$. The normalization of the mode is done as in [35], but since the plane wave extends infinitely in the (x,y) plane, we evaluate the integral over a normalization area A. We thus construct a full solution for the asymptotic-in field according to

$$\mathbf{D}_{Rk}^{asy\text{-}in}(\mathbf{r}) = \sqrt{\frac{\epsilon_0 n_R^2(\omega_{Rk})}{2\pi A}\frac{v_{gR}(\omega_{Rk})}{v_{pR}(\omega_{Rk})}}\frac{n^2(z,\omega_{Rk})}{n_R^2(\omega_{Rk})}\mathbf{f}_{Rk}(-z), \tag{56}$$

where $\mathbf{f}_{Rk}(-z)$ is a dimensionless function of just the z coordinate, which can be easily evaluated for an arbitrary multilayer using the well-known transfer matrix method [47] and describes the electric field along the multilayer. Note that quantities such as the refractive indices n as well as the group v_g and phase v_p velocities carry the channel labels R and L, as the left and right channels are not, in general, identical as they were for the microring considered above. A similar construction follows for $[\mathbf{D}_{Lk}^{asy\text{-}out}]^*$. The nonlinear coupling parameter is now

$$S_{L;RR}(k,k_1,k_2) = \frac{\overline{\chi}_2}{(2\pi c A)^{3/2}}\sqrt{\frac{v_{gL}(\omega_{Lk})v_{gR}(\omega_{Rk_1})v_{gR}(\omega_{Rk_2})}{\epsilon_0 n_L(\omega_{Lk})n_R(\omega_{Rk_1})n_R(\omega_{Rk_2})}} \times \sqrt{\frac{(\hbar\omega_{Lk})(\hbar\omega_{Rk_1})(\hbar\omega_{Rk_2})}{8}} J_{L;RR}(k,k_1,k_2) \times \int_A dx\, dy, \tag{57}$$

where $\overline{\chi}_2$ is a reference susceptibility value introduced solely for convenience, and

$$J_{L;RR}(k,k_1,k_2) = \int dz \frac{\chi_2^{ijk}(z)}{\overline{\chi}_2} f_{Lk}^i(z) f_{Rk_1}^j(-z) f_{Rk_2}^k(-z) \tag{58}$$

is a function that describes the field overlap integral and contains all of the information regarding the structure.

Following [35] we can now obtain the expression for the wave function of the generated state (see the Appendix). In particular, if the pump is a coherent state with a very general wave form $\tilde{\phi}_P(\omega)$, we have

$$\tilde{\phi}_{L;RR}(\omega) = \frac{i}{\hbar}\frac{2\pi\alpha^2}{\beta}\int d\omega_1 d\omega_2 \frac{\tilde{\phi}_P(\omega_1)\tilde{\phi}_P(\omega_2)S_{L;RR}(k_L(\omega),k_R(\omega_1),k_R(\omega_2))\delta(\omega-\omega_1-\omega_2)}{\sqrt{v_{g_L}(\omega)v_{g_R}(\omega_1)v_{g_R}(\omega_2)}}, \tag{59}$$

where $|\alpha|^2$ and $|\beta|^2$ are the expectation values of the numbers of pump and generated photons, respectively. By integrating over ω_2 and using (57) we get

$$\tilde{\phi}_{L;RR}(\omega) = \frac{2\pi\alpha^2}{\beta}\frac{1}{\sqrt{A}}\frac{\bar{\chi}_2}{(4\pi c)^{3/2}}\frac{i}{\sqrt{\epsilon_0 n_L(\omega)}}\sqrt{\hbar\omega}\int d\omega_1\sqrt{\frac{\omega_1(\omega-\omega_1)}{n_R(\omega_1)n_R(\omega-\omega_1)}}\tilde{\phi}_P(\omega_1)\tilde{\phi}_P(\omega-\omega_1) \times J_{L;RR}(k_L(\omega),k_R(\omega_1),k_R(\omega-\omega_1)). \tag{60}$$

As usual, $|\beta|^2$ is determined by requiring that $|\tilde{\phi}_{L;RR}(\omega)|^2$ is normalized.

It is interesting to study the case of a continuous wave (cw) pump at ω_p. To this end, we consider a pump pulse centered at ω_p having a rectangular shape in time of width ΔT:

$$\tilde{\phi}_P(\omega) = \sqrt{\frac{\Delta T}{2\pi}}\,\mathrm{sinc}\left(\frac{(\omega-\omega_p)\Delta T}{2}\right). \tag{61}$$

By inserting (62) in (60) and integrating $|\tilde{\phi}_P(\omega)|^2$ (see the Appendix), we get the number of generated photons. Then, since the pump and SHG intensities are

$$I(\omega_p) = \frac{|\alpha|^2\hbar\omega_p}{A\Delta T}, \qquad I(2\omega_p) = \frac{|\beta|^2 2\hbar\omega_p}{A\Delta T}, \tag{62}$$

we have that as $\Delta T \to \infty$ the multilayer nonlinear transmittance is

$$T^{NL}(\omega_p) = \frac{I(2\omega_p)}{I^2(\omega_p)} = \frac{\omega_p^2\bar{\chi}_2^2}{2\epsilon_0 c^3 n_L(2\omega_p)n_R^2(\omega_p)} \times |J_{L;RR}(k_L(2\omega_p),k_R(\omega_p),k_R(\omega_p))|^2. \tag{63}$$

One can immediately verify that, in the case of a homogeneous and isotropic medium of length L and susceptibility $\bar{\chi}_2$, (64) gives the usual classical result [48]. More importantly, the calculation of the cw SH nonlinear transmittance of an arbitrary multilayer is now straightforward, as it is reduced to the evaluation of the field overlap integral (58).

We consider a specific one-dimensional photonic crystal studied earlier [45], in which both the pump and the second-harmonic fields are resonant with a photonic band edge. This structure is particularly interesting, as it can demonstrate SHG efficiency that scales with the eighth power of the crystal length. Surprisingly, this occurs without realizing the well-known phase-matching condition.

The structure consists of $Al_{0.25}Ga_{0.75}As/Alo_x$ stacks with layer thicknesses $L_1 = L_2 = 373$ nm. We assume that the multilayer is oriented along the [111] direction, ensuring that the $\chi^{(2)}$ susceptibility tensor has a nonzero response for a pump at normal incidence, and for simplicity take both the left and right channel materials to be air. The structure is designed to have a doubly resonant condition between the band-edge resonances of the II and IV photonic gaps [45], with the fundamental resonance at 0.62 eV ($\simeq 2\ \mu$m). For a pump narrowly centered at this energy, we expect a scaling of the SHG intensity proportional to N^8, N being the number of periods. This scaling is due in part to the total field enhancement at the band edge, which accounts for N^6 (N^4 for the fundamental field and N^2 at the second harmonic), and in part due to the fact that the structure is shorter than the SHG coherence length, which is proportional to N. This gives an additional contribution of N^2 [45]. The calculated nonlinear transmittance as a function of N is shown in Fig. 6.

Next we want to consider the case of SPDC in a generic multilayer when the pump pulse is at normal incidence on the left side of the multilayer and the generated photon pairs emerge from the right side of the structure and propagate collinearly with the pump (see Fig. 5). Under these assumptions, the process is opposite to the SHG process discussed above, and exactly the same as the SPDC process discussed in Sec. V.

Indeed, starting from (41) and (42), and using (56) we can derive the biphoton wave function following the same procedure used in the previous section for the ring, and find

$$\tilde{\phi}_{RR;L}(\omega_1,\omega_2) = \frac{2\pi\sqrt{2}\alpha}{\beta}\frac{i}{\hbar}\frac{1}{c^{3/2}}\tilde{\phi}_P(\omega_1+\omega_2) \times S_{RR;L}(k_R(\omega_1),k_R(\omega_2),k_L(\omega_1+\omega_2)), \tag{64}$$

where $|\alpha|^2$ and $|\beta|^2$ are the expectation values of the number of pump photons and generated pairs, respectively, $\tilde{\phi}_P(\omega)$ is the normalized pump pulse wave form and $S_{RR:L}(\omega_1,\omega_2,\omega)$ is a function that depends on the field overlap integral defined by analogy with (57). One can immediately verify that

$$S_{RR;L}(k_R(\omega_1),k_R(\omega_2),k_L(\omega)) = S_{L;RR}(k_L(\omega),k_R(\omega_1),k_R(\omega_2)). \tag{65}$$

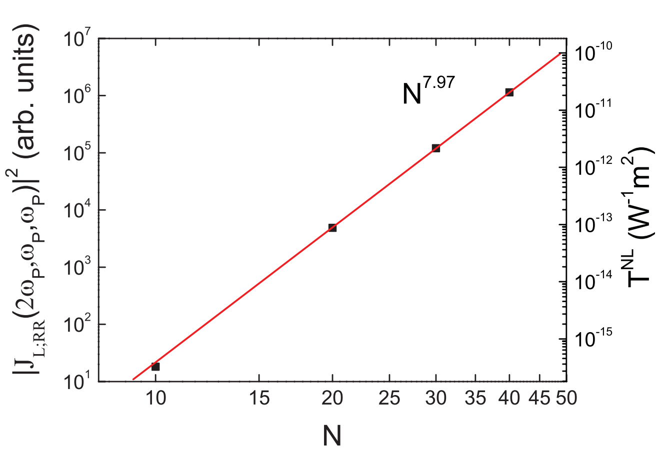

FIG. 6. (Color online) Calculated nonlinear transmittance and overlap integral in (64) as a function of the number, N, of periods of the structure.

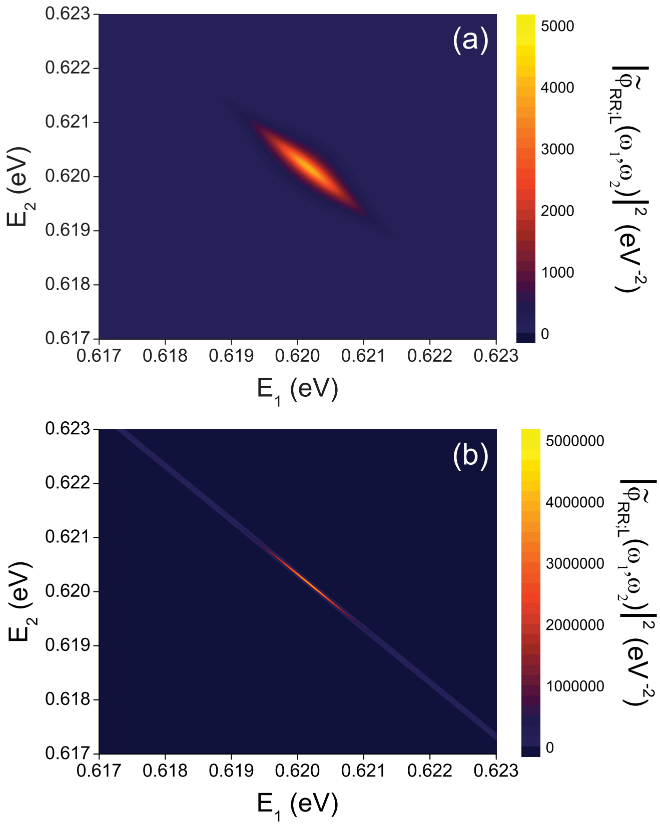

FIG. 7. (Color online) Biphoton probability densities for a structure with $N = 20$ periods. The pump pulses are tuned at the second-harmonic band edge with durations of (a) $\Delta T = 1$ ps and (b) $\Delta T = 1$ ns.

This is clear by constructing the fields in terms of the asymptotic-in and -out fields and remembering that we are considering the opposite process of SHG in a configuration where the photons' propagation directions are inverted.

As an example, in Fig. 7 we show two normalized biphoton probability densities describing photon pairs generated in the multilayer described. We consider $N = 20$ periods and a pump pulse centered at 1.24 eV with a spectral shape described by (62). We calculate the biphoton probability density for a short ($\Delta T = 1$ ps) and a long ($\Delta T = 1$ ns) pulse. In analogy with what was reported in [17] for ring resonators, the shape of the biphoton probability density, and thus the photons' correlation, strongly depends on the pulse duration, which controls the spectral width of the pulse. The longer the pulse, the greater the correlation between two photons of a generated pair, due to a tighter restriction on energy conservation. A detailed discussion of this example is beyond the scope of this paper, but we intend to come back to this interesting problem in a future communication.

VII. CONCLUSIONS

In problems in linear and nonlinear optics where a full quantum treatment is desired, often the first step is the identification of an appropriate Hamiltonian. Even that can be challenging. In artificially structured materials with cavities, one strategy is to build a Gardiner-Collect-type Hamiltonian, with coupling between external modes and effective cavity modes. But for many structures the identification of the effective cavity modes and a rigorous description of the coupling with the external modes is difficult or impossible. We have presented a way to bypass this problem which is applicable to a large variety of photonic systems, from integrated circuits to layered structures. It exploits *asymptotic-in* and *asymptotic-out* fields, in close analogy with scattering theory in quantum mechanics. These fields are the stationary solutions of the classical linear Maxwell equations, and can be evaluated analytically or numerically. We demonstrated in Sec. II that such solutions can be used to describe the electromagnetic field in either a classical or a quantum framework, and so from the results of classical calculations it is possible to construct an appropriate Hamiltonian associated with the problem of interest. In particular, in Sec. III we showed that the linear scattering problem can be viewed as a basis transformation from that of asymptotic-in fields to that of asymptotic-out fields. In Sec. IV we applied this strategy to the description of scattering in the presence of nonlinearities, and in Secs. V and VI we presented two examples of the inclusion of a second-order nonlinear optical response within our formalism. In the first example of a side-coupled ring resonator, we calculated the SPDC conversion efficiency and obtained an expression identical to that reported earlier on the basis of a Gardiner-Collett Hamiltonian. In the second example of an arbitrary multilayer structure, we derived an expression for the cw SHG nonlinear transmittance in a manner much simpler than that of previous calculations and studied SPDC in such a structure, calculating the biphoton wave function associated with the state of the generated photons.

These examples illustrate the versatility of our approach. They show how our strategy leverages solutions of the classical linear Maxwell equations, found either analytically or numerically, to simplify the solution of nonlinear classical or quantum problems. They also show how it highlights the physics of the nonlinear interaction and its enhancement in cavity structures. Thus it should be particularly useful not only for obtaining quantitative predictions, but as well for achieving a better understanding of the physics behind the phenomena.

ACKNOWLEDGMENTS

This work is supported by the Italian Ministry of University and Research, FIRB Contract No. RBFR08QIP5, the foundation Alma Mater Ticinensis, and by the Natural Science and Engineering Research Council of Canada.

APPENDIX

Here we derive the expression of the nonlinear transmittance in the case of an arbitrary multilayer under the assumptions discussed in Sec. VI. This can be done by following the backward Heisenberg picture approach [35] and considering the nonlinear Hamiltonian given by (53) and (57). Although the approach is quite similar to that for determining the SPDC efficiency [35], there are some subtleties worth noting.

We take our asymptotic-in ket (37) to be a coherent state

$$|\psi_{in}\rangle = e^{\alpha A_P^\dagger - \text{H.c.}}|\text{vac}\rangle,$$

where

$$A_P^\dagger = \int dk\, \phi_P(k) a_{Rk}^\dagger,$$

$a_{Rk}^\dagger$ is the creation operator associated with a photon coming from the right channel having momentum k, and the pump pulse wave form $\phi_P(k)$ is normalized according to

$$\int dk |\phi_P(k)|^2 = 1.$$

Alternatively, we may write

$$\tilde{\phi}_P(\omega) = \sqrt{\frac{dk(\omega)}{d\omega}}\phi_P(k(\omega)) = \sqrt{\frac{1}{v_{g_R}(\omega)}}\phi_P(k(\omega)), \quad \text{(A1)}$$

where $v_{g_R}(\omega)$ is the group velocity in the right channel; a corresponding prefactor is introduced for the left channel so all pump and generated photon wave functions are appropriately normalized.

Using (39), the asymptotic-out ket (38) can be written

$$|\psi_{out}\rangle = e^{\alpha \overline{A}_P^\dagger(t_0) - \text{H.c.}}|\text{vac}\rangle,$$

where

$$\overline{A}_P^\dagger(t_0) = \int dk_1 \phi_P(k_1)\overline{a}_{Rk_1}^\dagger(t_0)$$

is a backward Heisenberg operator [35], and $\overline{a}_{Rk_1}^\dagger(t)$ satisfies

$$i\hbar\frac{d\overline{a}_{Rk_1}^\dagger(t)}{dt} = 2\int dk_2 dk S_{L;RR}(k,k_1,k_2;t)\overline{b}_{Lk}^\dagger(t)\overline{a}_{Rk_2}(t), \quad \text{(A2)}$$

with

$$S_{L;RR}(k,k_1,k_2;t) = S_{L;RR}(k,k_1,k_2)e^{i(\omega-\omega_1-\omega_2)t}. \quad \text{(A3)}$$

Equation (A2) has the zeroth-order solution

$$[\overline{a}_{Rk_1}^\dagger(t)]^0 = \overline{a}_{Rk_1}^\dagger(t_1) = a_{Rk_1}^\dagger,$$

and thus, in the limit of an undepleted pump, we have

$$\begin{aligned}\overline{a}_{Rk_1}^\dagger(t) &= a_{Rk_1}^\dagger + \frac{2}{i\hbar}\int dk_2 dk \left[\int_{t_1}^{t_0} dt S_{L;RR}(k,k_1,k_2;t)\right]\overline{b}_{Lk}^\dagger \overline{a}_{Rk_2} \\ &= a_{Rk_1}^\dagger + \frac{4\pi i}{\hbar}\int dk_2 dk S_{L;RR}(k,k_1,k_2) b_{Lk}^\dagger a_{Rk_2}\delta(\omega_{Lk}-\omega_{Rk_1}-\omega_{Rk_2}),\end{aligned}$$

where we have extended the range of integration from $t_0 \to -\infty$ to $t_1 \to \infty$.

In writing the final form of the asymptotic-out ket, there is an additional subtlety that arises for SHG compared to SPDC [35]—namely, that not all of the operators in the exponential commute with each other. Thus, following

$$e^{A+B} = e^A e^{-\frac{1}{2}[A,B]+\text{higher-order terms}} e^B, \quad \text{(A4)}$$

where any one of the "higher-order terms" is proportional to

$$[S_1,[S_2,\cdots[S_{n-1},S_n]\cdots]],\ S_{i=1,2,\ldots,n} = A \text{ or } B,$$

we take

$$\begin{aligned}A &= \alpha\int dk_1\phi_P(k_1)a_{Rk_1}^\dagger - \text{H.c.},\\ B &= \frac{4\pi i\alpha}{\hbar}\int dk dk_1 dk_2 \phi_P(k_1)S_{L;RR}(k,k_1,k_2)b_{Lk}^\dagger a_{Rk_2} - \text{H.c.},\end{aligned} \quad \text{(A5)}$$

and work out

$$-\frac{1}{2}[A,B] = \frac{2\pi i\alpha^2}{\hbar}\int dk\, dk_1 dk_2 \phi_P(k_1)\phi_P(k_2) \times S_{L;RR}(k,k_1,k_2)b_{Lk}^\dagger - \text{H.c.}$$

Note that from (A5) we have

$$e^B|\text{vac}\rangle = |\text{vac}\rangle.$$

Then, neglecting the higher-order terms mentioned above, as they either contain higher powers of the (assumed small) nonlinearity or involve back-action on the pump (and thus violate the undepleted pump approximation), we can write the asymptotic-out ket as

$$|\psi_{out}\rangle = e^{(\alpha A_P^\dagger + \beta C^\dagger)-\text{H.c.}}|\text{vac}\rangle,$$

where

$$C^\dagger = \int dk\, \phi_{L;RR}(k)b_{Lk}^\dagger$$

is the creation operator describing the generated photons exiting to the left side of the multilayer, and

$$\phi_{L;RR}(k) = \frac{2\pi\alpha^2}{\beta}\frac{i}{\hbar}\int dk_1 dk_2 \phi_P(k_1)\phi_P(k_2) \times S_{L;RR}(k,k_2,k_1)\delta(\omega_{Lk}-\omega_{Rk_1}-\omega_{Rk_2})$$

is the generated photon wave function, with β chosen such that it is normalized. This allows us to identify $|\beta|^2$ with the expectation value of the number of generated photons. Using $(A1)$, we can now write the photon wave function in terms of frequency and, integrating over ω_2, obtain (60). The number of generated photons is given by

$$|\beta|^2 = \frac{|\alpha|^2}{A}\frac{\bar{\chi}_2^2}{16\pi c^3\epsilon_0}\int_0^\infty \frac{\hbar\omega}{n_L(\omega)}\left|\int_0^\infty d\omega_1\sqrt{\frac{\omega_1(\omega-\omega_1)}{n_R(\omega_1)n_R(\omega-\omega_1)}}\tilde{\phi}_P(\omega_1)\tilde{\phi}_P(\omega-\omega_1)J_{L;RR}(k_L(\omega),k_R(\omega_1),k_R(\omega-\omega_1))\right|^2. \tag{A6}$$

To calculate the multilayer cw nonlinear transmittance we consider a pump pulse (61).

Due to the spectral shape of the pulse, for a sufficiently large ΔT, the integrand in the modulus is significantly different from zero when

$$\omega_1 - \omega_p \simeq 0, \tag{A7}$$

$$\omega - \omega_1 - \omega_p \simeq 0. \tag{A8}$$

Thus, neglecting material dispersion over the pump bandwidth, and taking all the slowly varying functions in ω_1 and $\omega - \omega_1$ as constant, we have

$$\begin{aligned}|\beta|^2 = {}& \frac{|\alpha|^4}{A}\frac{\bar{\chi}_2^2}{16\pi c^3\epsilon_0}\int_0^\infty d\omega\frac{\omega_p^2}{n_R^2(\omega_p)}\frac{\hbar\omega}{n_L(\omega)}|J_{L;RR}(k_L(\omega),k_R(\omega_p),k_R(\omega-\omega_p))|^2\frac{\Delta T^2}{4\pi^2}\\ &\times\left|\int_0^\infty d\omega_1 \mathrm{sinc}\left(\frac{(\omega_1-\omega_p)\Delta T}{2}\right)\mathrm{sinc}\left(\frac{(\omega_1-\omega_p-\omega+2\omega_p)\Delta T}{2}\right)\right|^2.\end{aligned} \tag{A9}$$

For the same reasons, when ΔT is sufficiently large, we can extend the integral within the modulus in the range $(-\infty,\infty)$, the integrand being negligible in the $(-\infty,0)$ interval. Then, using the result

$$\int_{-\infty}^{+\infty} dx\, \mathrm{sinc}(xa)\mathrm{sinc}[(x-\tilde{x})a] = \frac{\pi}{a}\mathrm{sinc}(\tilde{x}a), \tag{A10}$$

we have

$$\begin{aligned}|\beta|^2 &= \frac{|\alpha|^4}{A}\frac{\bar{\chi}_2^2}{16\pi c^3\epsilon_0}\int_0^\infty d\omega\frac{\omega_p^2}{n_R^2(\omega_p)}\frac{\hbar\omega}{n_L(\omega)}|J_{L;RR}(k_L(\omega),k_R(\omega_p),k_R(\omega_p))|^2\frac{\Delta T^2}{4\pi^2}\left|\frac{2\pi}{\Delta T}\mathrm{sinc}\left(\frac{(\omega-2\omega_p)\Delta T}{2}\right)\right|^2\\ &= \frac{|\alpha|^4}{A}\frac{\bar{\chi}_2^2}{16\pi c^3\epsilon_0}\int_0^\infty d\omega\frac{\omega_p^2}{n_R^2(\omega_p)}\frac{\hbar\omega}{n_L(\omega)}|J_{L;RR}(k_L(\omega),k_R(\omega_p),k_R(\omega_p))|^2\left|\mathrm{sinc}\left(\frac{(\omega-2\omega_p)\Delta T}{2}\right)\right|^2.\end{aligned} \tag{A11}$$

Again, this last integrand is significantly different from zero when $\omega \simeq 2\omega_p$. This leads to

$$\begin{aligned}|\beta|^2 &= \frac{|\alpha|^4}{A}\frac{\bar{\chi}_2^2}{16\pi c^3\epsilon_0}\frac{2\hbar\omega_p^3}{n_R^2(\omega_p)n_L(2\omega_p)}|J_{L;RR}(k_L(2\omega_p),k_R(\omega_p),k_R(\omega_p))|^2\int_0^\infty d\omega\left|\mathrm{sinc}\left(\frac{(\omega-2\omega_p)\Delta T}{2}\right)\right|^2,\\ &= \frac{|\alpha|^4}{A\Delta T}\frac{\bar{\chi}_2^2}{16c^3\epsilon_0}\frac{4\hbar\omega_p^3}{n_R^2(\omega_p)n_L(2\omega_p)}|J_{L;RR}(k_L(2\omega_p),k_R(\omega_p),k_R(\omega_p))|^2.\end{aligned} \tag{A12}$$

Finally, using (A12) and (62), we obtain (63).

[1] T. Baba, Nat. Photonics **2**, 465 (2008).
[2] M. Hafezi, E. A. Demler, M. D. Lukin, and J. M. Taylor, Nat. Physics **7**, 907 (2011).
[3] E. Purcell, Phys. Rev. **69**, 681 (1946).
[4] V. R. Almeida and M. Lipson, Opt. Lett. **29**, 2387 (2004).
[5] H. M. Gibbs, *Optical Bistability: Controlling Light with Light* (Academic Press, Orlando, FL, 1985).
[6] T. Tanabe, M. Notomi, S. Mitsugi, A. Shinya, and E. Kuramochi, Appl. Phys. Lett. **87**, 151112 (2005).
[7] M. Belotti, M. Galli, D. Gerace, L. C. Andreani, G. Guizzetti, A. R. Md Zain, N. P. Johnson, M. Sorel, and R. M. De La Rue, Opt. Express **18**, 1450 (2010).
[8] Y. H. Wen, O. Kuzucu, T. Hou, M. Lipson, and A. L. Gaeta, Opt. Lett. **36**, 1413 (2011).
[9] M. W. McCutcheon, J. F. Young, G. W. Rieger, D. Dalacu, S. Frederick, P. J. Poole, and R. L. Williams, Phys. Rev. B **76**, 245104 (2007).
[10] K. Rivoire, Z. Lin, F. Hatami, W. T. Masselink, and J. Vuckovic, Opt. Express **17**, 22609 (2009).
[11] M. Galli, D. Gerace, K. Welna, T. F. Krauss, L. O'Faolain, G. Guizzetti, and L. C. Andreani, Opt. Express **18**, 16613 (2010).
[12] J. S. Levy, M. A. Foster, A. L. Gaeta, and M. Lipson, Opt. Express **19**, 11415 (2011).
[13] M. Hossein-Zadeh and K. J. Vahala, IEEE J. Sel. Top. Quantum Electron. **16**, 276 (2010).
[14] B. Corcoran, C. Monat, C. Grillet, D. J. Moss, B. J. Eggleton, T. P. White, L. O'Faolain, and T. F. Krauss, Nat. Photonics **3**, 206 (2009).
[15] Z. Yang and J. E. Sipe, Opt. Lett. **32**, 3296 (2007).

[16] S. Clemmen, K. Phan Huy, W. Bogaerts, R. G. Baets, Ph. Emplit, and S. Massar, Opt. Express **17**, 16558 (2009).
[17] L. G. Helt, Z. Yang, M. Liscidini, and J. E. Sipe, Opt. Lett. **35**, 3006 (2010).
[18] L. G. Helt, M. Liscidini, A. Farsi, S. Clemmen, V. Venkataraman, J. S. Levy, M. Lipson, A. L. Gaeta, and J. E. Sipe, in *Quantum Electronics and Laser Science Conference, OSA Technical Digest (CD)* (Optical Society of America, Baltimore, Maryland, 2011), paper QWA4.
[19] C. Xiong, C. Monat, A. S. Clark, C. Grillet, G. D. Marshall, M. J. Steel, J. Li, L. O'Faolain, T. F. Krauss, J. G. Rarity, and B. J. Eggleton, Opt. Lett. **36**, 3413 (2011).
[20] S. M. Dutra, *Cavity Quantum Electrodynamics: The Strange Theory of Light in a Box* (John Wiley & Sons, Hoboken, NJ, 2004).
[21] C. W. Gardiner and M. J. Collett, Phys. Rev. A **31**, 3761 (1985).
[22] J. E. Heebner, R. Grover, and T. Ibrahim, *Optical Microresonators: Theory, Fabrication, and Applications* (Springer, London, 2008).
[23] See, e.g., B. J. Dalton, S. M. Barnett, and P. L. Knight, J. Mod. Opt. **46**, 1315 (1999); B. J. Dalton and P. L. Knight, *ibid*. **46**, 1817 (1999).
[24] G. Breit and H. A. Bethe, Phys. Rev. **93**, 888 (1954).
[25] J. R. Taylor, *Scattering Theory: The Quantum Theory of Nonrelativistic Collisions* (John Wiley & Sons, New York, 1972).
[26] R. Graham, Z. Phys. B **76**, 265 (1989).
[27] S. Fan, S. E. Kocabasü, and J.-T. Shen, Phys. Rev. A **82**, 063821 (2010).
[28] See, e.g., Yoseph Imry, *Introduction to Mesoscopic Physics* (Oxford University Press, New York, 1997).
[29] J. E. Sipe, N. A. R. Bhat, P. Chak, and S. Pereira, Phys. Rev. E **69**, 016604 (2004).
[30] N. A. R. Bhat and J. E. Sipe, Phys. Rev. A **73**, 063808 (2006).
[31] A. Gondarenko, J. S. Levy, and M. Lipson, Opt. Express **17**, 11366 (2009).
[32] J. S. Levy, A. Gondarenko, M. A. Foster, A. C. Turner-Foster, A. L. Gaeta, and M. Lipson, Nat. Photonics **4**, 37 (2010).
[33] A. Faraon, P. E. Barclay, C. Santori, K.-M. C. Fu, and R. G. Beausoleil, Nat. Photonics **5**, 301 (2011).
[34] N. Vermeulen, J. E. Sipe, Y. Lefevre, C. Debaes, and H. Thienpont, IEEE J. Sel. Top. Quantum Electron. **17**, 1078 (2011).
[35] Z. Yang, M. Liscidini, and J. E. Sipe, Phys. Rev. A **77**, 033808 (2008).
[36] J. Trull, R. Vilaseca, J. Martorell, and R. Corbalán, Opt. Lett. **20**, 1746 (1995).
[37] M. Scalora, M. J. Bloemer, A. S. Manka, J. P. Dowling, C. M. Bowden, R. Viswanathan, and J. W. Haus, Phys. Rev. A **56**, 3166 (1997).
[38] M. Centini, M. Centini, C. Sibilia, M. Scalora, G. D'Aguanno, M. Bertolotti, M. J. Bloemer, C. M. Bowden, and I. Nefedov, Phys. Rev. E **60**, 4891 (1999).
[39] Y. Dumeige, I. Sagnes, P. Monnier, P. Vidakovic, I. Abram, C. Mériadec, and A. Levenson, Phys. Rev. Lett. **89**, 043901 (2002).
[40] M. Centini, M. Centini, G. D'Aguanno, L. Sciscione, C. Sibilia, M. Bertolotti, M. Scalora, and M. J. Bloemer, Opt. Lett. **29**, 1924 (2004).
[41] M. Liscidini and L. C. Andreani, Appl. Phys. Lett. **85**, 1883 (2004).
[42] T. Ochiai and K. Sakoda, Opt. Express **13**, 9094 (2005).
[43] M. Liscidini and L. C. Andreani, Phys. Rev. E **73**, 016613 (2006).
[44] X. Vidal and J. Martorell, Phys. Rev. Lett. **97**, 013902 (2006).
[45] M. Liscidini, A. Locatelli, L. C. Andreani, and C. De Angelis, Phys. Rev. Lett. **99**, 053907 (2007).
[46] Y. Sheng, D. Ma, M. Ren, W. Chai, Z. Li, K. Koynov, and W. Krolikowski, Appl. Phys. Lett. **99**, 031108 (2011).
[47] A. Yariv and P. Yeh, *Optical Waves in Crystals* (John Wiley & Sons, New York, 2003).
[48] Y. R. Shen, *Principles of Nonlinear Optics* (John Wiley & Sons, New York, 2003).